crystals

MDPI

Article

Syzygium aromaticum Bud Extracted Core–Shell Ag–Fe Bimetallic Nanoparticles: Phytotoxic, Antioxidant, Insecticidal, and Antibacterial Properties

Farah Murtaza [1], Naseem Akhter [1,*], Muhammad Azam Qamar [2,*], Asma Yaqoob [3], Anis Ahmad Chaudhary [4], Bhagyashree R. Patil [5], Salah Ud-Din Khan [6], Nasir Adam Ibrahim [4], Nosiba S. Basher [4], Mohammed Saad Aleissa [4], Iqra Kanwal [1] and Mohd Imran [7]

1 Department of Chemistry, The Government Sadiq College Women's University Bahawalpur, Bahawalpur 63100, Pakistan; ifrach231@gmail.com (F.M.)
2 Department of Chemistry, School of Science, University of Management and Technology, Lahore 54770, Pakistan
3 Institute of Biochemistry Biotechnology and Bioinformatics, The Islamia University of Bahawalpur, Bahawalpur 63100, Pakistan; asma.yaqoob@iub.edu.pk
4 Department of Biology, College of Science, Imam Mohammad Ibn Saud Islamic University (IMSIU), Riyadh 11623, Saudi Arabia; naabdlneim@imamu.edu.sa (N.A.I.); nsbasher@imamu.edu.sa (N.S.B.)
5 Department of Biology, College of Science, Jazan University, Jizan 45142, Saudi Arabia
6 Department of Biochemistry, College of Medicine, Imam Mohammad Ibn Saud Islamic University (IMSIU), Riyadh 11623, Saudi Arabia
7 Department of Chemical Engineering, College of Engineering, Jazan University, P.O. Box 706, Jazan 45142, Saudi Arabia; malain@jazanu.edu.sa
* Correspondence: drnaseem@gscwu.edu.pk (N.A.); s2016263001@post.umt.edu.pk (M.A.Q.)

check for updates

Citation: Murtaza, F.; Akhter, N.; Qamar, M.A.; Yaqoob, A.; Chaudhary, A.A.; Patil, B.R.; Khan, S.U.-D.; Ibrahim, N.A.; Basher, N.S.; Aleissa, M.S.; et al. *Syzygium aromaticum* Bud Extracted Core–Shell Ag–Fe Bimetallic Nanoparticles: Phytotoxic, Antioxidant, Insecticidal, and Antibacterial Properties. *Crystals* **2024**, *14*, 510. https://doi.org/10.3390/cryst14060510

Academic Editor: Leonid Kustov

Received: 29 March 2024
Revised: 14 May 2024
Accepted: 21 May 2024
Published: 27 May 2024

Abstract: Today, there is the roar of sustainable material development around the globe. Green nanotechnology is one of the extensions of sustainability. Due to its sustainable approach, the green fabrication of nanoparticles has recently surpassed their classical synthesis in popularity. Among metal nanoparticles, contemporary findings have demonstrated that bimetallic nanoparticles possess more potential for different applications than monometallic nanoparticles due to the synergistic effects of the two metals. So, we are presenting facile, one-vessel, and one-step phyto-fabrication of Ag–Fe BMNPs using the bud extract of Syzygiumaromaticum. The synthesized nanoparticles were characterized by UV-VIS, XRD, EDX, FTIR, and SEM. The synthesized NPs and the extract underwent biological studies. The radical scavenging potential of the NPs and the extract was found to be 64% and 73%, and the insecticidal potential was found to be 80% and 100%, respectively. Similarly, the NPs and the extract both exhibited good antibacterial activity. The zone of inhibition using 100 mg/mL of extract and NPs was found to be 1 cm against all bacterial species, i.e., *K. pneumonia*, *E. coli*, and *S. aureus*. It was 1.5 cm, 1.3 cm, and 1 cm against *K. pneumonia*, *E. coli*, and *S. aureus*, respectively, showing that the antibacterial activity of the extract is higher than that of the NPs. So, this study unlocks the synthesis of Ag–Fe bimetallic nanoparticles using eco-safe, cost-effective, facile, and least-harmful green methodology with potential applications of both NPs and SA extract in medical and agricultural fields, a step towards sustainability.

Keywords: sustainable development; Ag–Fe bimetallic nanoparticles; syzygiumaromaticum; antioxidant; antibacterial

1. Introduction

Nanotechnology is a progressing field of study that focuses on manipulating matter at the nanoscale to develop novel materials, devices, and systems with distinct features and functions [1,2]. These days, nanotechnology is shifting from one futuristic paradigm to another. The fields of sustainable nanotechnology include green synthesis and green

nanotechnology as a whole. The difficulties, goals, and complexity of scientific studies in green nanotechnology are opening up new avenues for advancements in both fields [3]. To attain sustainability, green nanotechnology involves the synthesis of nanoparticles (NPs) from natural bio-reductants present in plants, micro-organisms, and diverse bio-wastes [4].

Many different types of materials can be used to construct nanoparticles, including ceramics [5], metals [6], polymers [7,8], hydrogels [8,9], and semiconductors [10,11]. These materials have great potential in various domains including photocatalysis [12,13], energy storage [14], gas sensing [15], etc. Nanomaterials, which are so small that they are measured on the nanoscale, often have distinct physical, chemical, and biological characteristics that are distinct from those of their bulk counterparts. Numerous methods, including conventional and green, have been used to synthesize NPs [2,16]. In general, chemical processes are too expensive and involve the use of lethal and dangerous substances responsible for various problems, and physical methods of synthesizing NPs are expensive, expose workers to radiation, call for tremendous energy, temperature, and pressure, and produce a lot of trash [10]. In green nanotechnology, using poisonous materials and high temperatures, high pressures, or powers is unnecessary. In phytosynthesis, different biomolecules found in plant extracts act as phyto-stabilizers and phyto-reductants to synthesize NPs [17]. Such a protocol is inexpensive, straightforward, risk-free, benign, and eco-responsible. Photosynthesis of NPs is more prevalent than their synthesis using microorganisms, as plants are easily approachable, cost-effective, and easy to deal with [18]. Further, the preparation strategy using plants to get their extract is more facile than that for microorganisms as it is very difficult to maintain and handle their cultures. Moreover, diverse types of morphologies of NPs can be synthesized using plants due to the presence of biomolecules of diverse conformations in a vast variety of plants [2,19]. Metal-based nanoparticles (MNPs) are produced from metals in nano sizes. Highly electrically charged surfaces, different types of shapes, reactive properties, small pore sizes, colors, and responsiveness to natural factors like temperature, air, and solar radiation are just a few of these nanomaterials' distinctive qualities [20,21]. Among multifunctional nanoparticles, bimetallic nanoparticles (BMNPs) are the right mixture of two distinct metals with improved reaction characteristics [22]. Due to the combining effects of both metals compared to a single metal in monometallic nanoparticles (MMNPs), they have increased biological, catalytic, optical, magnetizing, and electronic properties. As a result, they have generated curiosity in research and applications in science [21]. Since BMNPs possess more physical characteristics than their monometallic counterparts, they also exhibit enhanced activities in various applications. They find applications in catalytic [23], sensing, antibacterial, antioxidant, anti-cancerous, etc., activities [24–26]. NPs are considered a crucial therapeutic tool because of their wide range of applications in therapies, such as disease identification, drug and gene transmission, tissue engineering, etc. [27]. MNPs' diminutive size makes it simple to enter and move around inside cells, where they perform biological tasks. Also, biomolecules present in the extract of plants have been extensively investigated, notably, polyphenols, like flavonoids and phenolic acids [28]. Flavonoids assist in boosting immunity, reducing inflammation, and protecting the body from free-radical damage. They oversee plants' antioxidant functions. These organic compounds have one or more OH groups attached to the aromatic ring of organic biomolecules. Numerous phytochemicals are in the outer leaves or under the bark [29]. They are unique to every plant, down to the individual plant cell. Some scientists also contend that combining phytochemicals and NPs of noble metals, like silver, lowers the risk of developing lung, breast, or colon cancer [30]. Synthesis of bimetallic silver–iron (Ag–Fe) nanoparticles is carried out by several methods including microwave-assisted, wet chemistry, and pulsed laser deposition, along with laser spray pyrolysis and liquid laser ablation methods, as the most effective approaches [31]. For example, the fabrication of Au–Ag nanoparticles by motor grinding by Murugadss and the preparation of Au–Pd nanoparticles under both hydrothermal conditions and microwave irradiation by Belousovd signifies the range of processes for creating bimetallic nanoparticles [32,33]. Although physical and chemical procedures are successful, they

are usually related to complex processes that can be costly and sometimes hazardous to the environment. On the contrary, the green synthesis approach primitively differs in the way natural compounds are applied as the reducing agents, thus rendering the whole process favorable to the environment. It is not only environmentally friendly but also fosters sustainability, which is the demand of the time for green technologies [34].

In Ag–Fe nanoparticles synthesis, we aim to take advantage of the distinct qualities of the metals—silver as an antimicrobial element and iron for its magnetic features. Indeed, these properties endow Ag–Fe nanoparticles with a wide spectrum of applications from catalysis and biomedicine to environmental remediation. This is the multifaceted nature of bimetallic nanoparticles. In this scenario, we underwent sustainable development of Ag–Fe BMNPs using bud extract of *Syzygium aromaticum*, also called clove, one of the most popular spices with built-in antimicrobial and radical scavenging properties. Its easy availability and low price make it a suitable candidate for sustainable development or green synthesis of NPs [35]. The use of *Syzygium aromaticum* bud extract in the manufacture of bimetallic nanoparticles (Ag–Fe) is a novel method that has not been documented before. A novel synthesis of bimetallic nanoparticles (Ag–Fe) using *Syzygium aromaticum* bud extract, a method not previously reported, is obtained. The extract and the NPs were also evaluated to estimate their antibacterial, antioxidant, and insecticidal potential. Lastly, a phytotoxic assessment of the NPs and the extract was also done to check their eco-toxicity.

2. Results

2.1. UV-VIS Analysis

Ag–Fe BMNPs gave their characteristic SPR peak cantered at 289 nm (Figure 1), which is in agreement with the previously reported work [36]. The UV–VIS range for Ag usually falls between 380 and 580 nm, while for Fe, it falls between 250 and 350 nm [36,37]. In the case of our BMNPs, the SPR peak at 289 nm (indicated by the arrow in Figure 1) comes within the UV–VIS range of Fe NPs, confirming the formation of the core–shell type of Ag–Fe BMNPs. BMNPs usually have three types of structure. They are alloy, heterogenous, and core–shell kind of structures. Different types of absorption bands are obtained depending upon the type of structures of BMNPs.

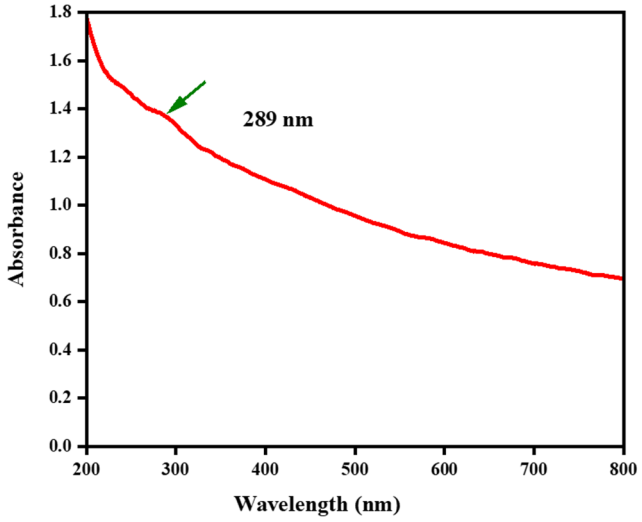

Figure 1. UV-Visible absorption spectra of Ag–Fe BMNPs.

In the case of heterogeneous materials, two absorption bands are formed. These bands contain the SPR peak, which is also referred to as the lambda maximum, in simpler terms, of each type of monometallic nanoparticle. One absorption band is formed in the case of a core–shell type of structure. This band is associated with the SPR peak of nanoparticles, which constitutes the outer shell of small metal nanoparticles (BMNPs). There is only

one absorption band that can be formed in an alloy structure, and that is the SPR peak that occurs at the wavelength range that falls between the wavelength ranges of individual monometallic nanoparticles on the spectrum. One type of metal serves as the core in the core–shell structure, while another type of metal is responsible for forming the shell. This sort of construction produces one absorption band with an SPR peak of nanoparticles that creates the outer surface of BMNPs, which is referred to as the shell of BMNPs. This structure fully masks the absorption band of the metal nanoparticles that constitute the interior structure, which is referred to as the core of BMNPs [38]. Since our absorption band resembles that of Fe NPs, it is a clear indication of a core–shell type of structure. Further, the full masking of the absorption band of Ag NPs and the damping in peak confirms the successful creation of core–shell Ag–Fe BMNPs, showing that Ag NPs are acting as the core, covered by Fe NPs as the shell. Similar results have been reported earlier in diverse types of BMNPs [39].

Synthetic Mechanism of Generation of Core–Shell Type of Structure

The reduction potential of metal ions contributes to the fabrication of such type of structure. Each metal ion has a different reduction potential. The metal ions present in metal's salt solution, having the greater reduction potential, possess the greater speed of reduction and, consequently, will reduce first and form the core, next to which the reduction of metal ions, having lesser reductional potential, occurs, which will develop the shell on the outer surface of the core. In the case of Ag–Fe core–shell BMNPs, the reduction potential of Ag is +0.80 V, and that of Fe is −0.04 V. So, Ag^{+1} ions were reduced first by biomolecules present in the SA extract, resulting in the core of Ag NPs, followed by the reduction of Fe^{+3}, forming the shell of Fe NPs [39,40].

2.2. FTIR Analysis

The major peaks in the FTIR spectrum of the bud extract, cantered at 3300 cm^{-1}, 2926 cm^{-1}, 1604 cm^{-1}, 1450 cm^{-1}–1640 cm^{-1}, 1049 cm^{-1} (Figure 2a), are due to stretching vibrations of O-H, C-H, C=O, C=C, C-O derivatives of carboxylic acids and O-H of eugenol, R-CH, aromatic alpha, beta ketones and esters, and R-CH_3, respectively [41,42]. The change in peak position and intensity of these absorption bands in the FTIR pattern of BMNPs indicates their role as bio-reductants and capping agents in the synthesis of NPs. Further, the small shift in peak position is also an indication that some of these biomolecules underwent slight changes in their structure, again confirming that they have been used in the bio-reduction process. The literature reveals that eugenol plays a significant role in synthesizing NPs whose O-H group oxidizes to the C=O group after removing electrons from itself. These electrons are used by metal ions, converting them into metallic form [43].

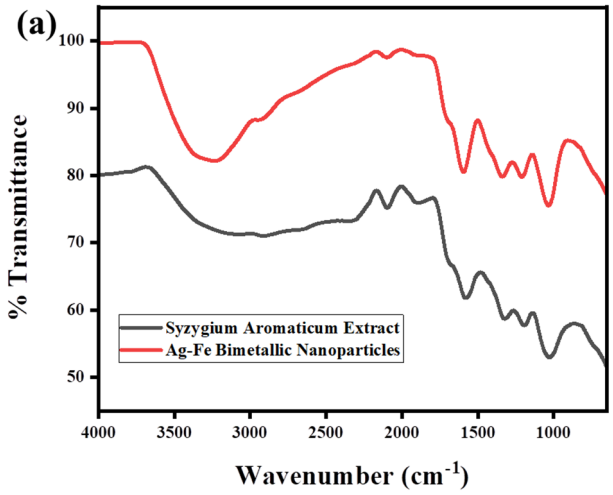

Figure 2. *Cont.*

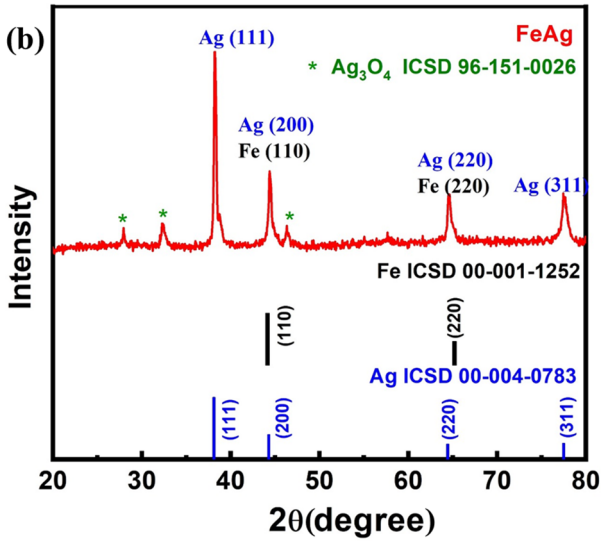

Figure 2. FTIR (**a**) and XRD (**b**) spectra of Ag–Fe BMNPs.

2.3. XRD Analysis

The XRD pattern of core–shell Ag–Fe BMNPs showed four major diffraction peaks at 2 theta values of 38.25°, 44.43°, 64.67°, and 77.59° (Figure 2b) that can be indexed at (111), (200) (110), (220) and (311) lattice planes, respectively, corresponding to JCPDS no. 00-004-0783 for Ag NPs and JCPDS card number 00-001-1252 for Fe NPs. Moreover, it was noticed that in case of FeAg alloy, the Fe and Ag peaks are merged and coexist at 65.186 for Fe and 64.428 for Ag, which can be supported by the JCPDS card number 658448 [44]. This demonstrates the face-centered cubic structure of Ag and Fe NPs, clearly emphasizing that the XRD pattern is made up of diffraction peaks of both Ag and Fe NPs, thus implying the formation of Ag–Fe BMNPs in very close accordance with already reported work [45]. As labelled with stars, the other three peaks suggest the presence of silver oxide impurities in small quantities [46].

2.4. SEM-EDX Analysis

The SEM image demonstrates that the shape of BMNPs is nearly spherical, and they are present in the form of a rough-surfaced small number of aggregates (Figure 3a) in exact agreement with the SEM image of Ag–Fe BMNPs [43]. This aggregation of particles clearly shows that NPs are beautifully stabilized and capped by phyto-molecules present in the SA extract. This aggregation most probably develops due to secondary forces of interaction between biomolecules serving as stabilizing agents on the surface of NPs [47]. The EDX peaks for Fe NPs are at 0.6, 6.4, and 7.1 KeV, while for Ag NPs they are at 3 KeV, which confirms the elemental make-up of Ag–Fe BMNPs (Figure 3b). The oxygen and carbon peaks suggest the presence of different phenolic compounds as bio-stabilizers on the surface of NPs, present on the shell of core–shell Ag–Fe BMNPs [48]. The other two peaks for calcium might represent an impurity due to the glass slide used for EDX characterization [49]. Moreover, the greater number of peaks of Fe NPs in contrast to Ag NPs confirms the core–shell structure of the as-prepared Ag–Fe BMNPs [50]. The atomic percentages (at. %) of Fe and Ag for Ag–Fe BMNPs obtained from EDX and ICP analysis are shown in Table 1. The result obtained from the ICP analysis is in good agreement with the values obtained from EDX.

Furthermore, the particle size of the nanoparticles is very important from the application point of view. The particle size of the nanoparticles in the current study was measured from the SEM image using Image J 1.52k software and the average particle size was observed 123 nm (Figure 3c).

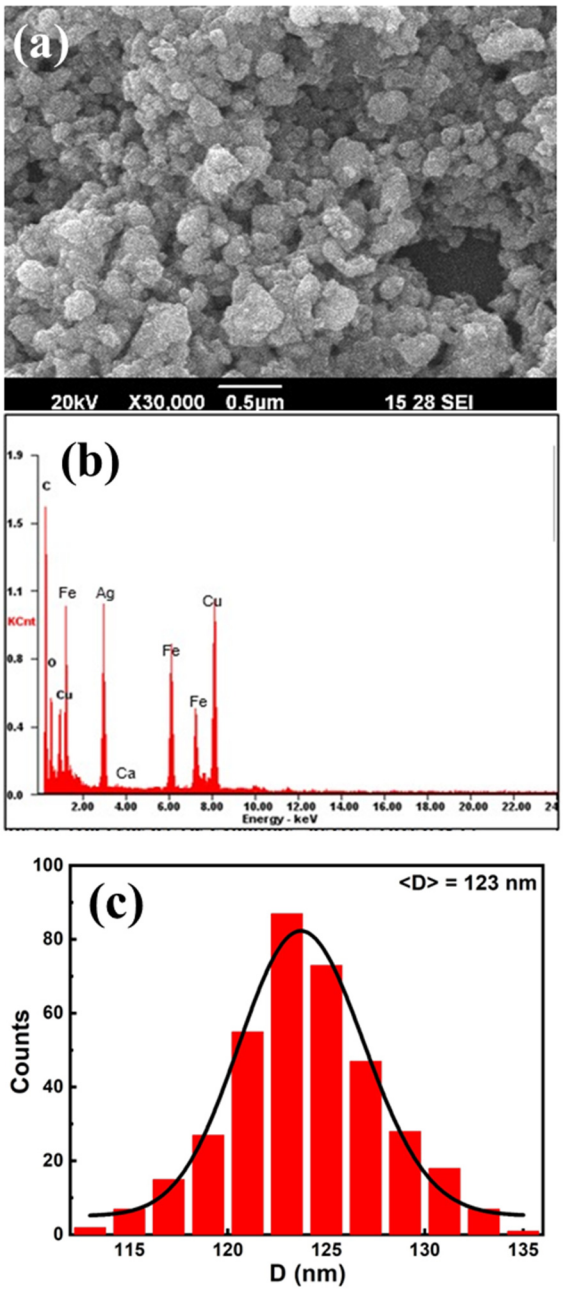

Figure 3. SEM (**a**) EDX spectra (**b**) and particle size distribution of Ag–Fe BMNPs (**c**).

Table 1. The atomic and weight % of Ag and Fe in Ag–Fe BMNPs.

Ag–Fe	Weight %		Atomic %	
	Ag (wt. %)	Fe (wt. %)	Ag (at. %)	Fe (at. %)
EDX	65.9	34.1	49.3	50
ICP			49.5	50

3. Discussion

3.1. Magnetic Studies

When an external magnetic field was applied to synthesize NPs, they became stuck to a magnetic chip (Figure 4), showing their magnetic properties and confirming the core–shell structure of synthesized BMNPs where Fe NPs were comprising the shells of BMNPs. Magnetic MNPs find extensive applications in medical fields. For example, they

are primarily used to diagnose and treat various diseases. In terms of diagnosis, they find imaging applications, such as MRI and sensing. They serve as multipurpose agents, like cell labeling, cell targeting, drug administration, and drug delivery. They are also used in cancer treatment, where they kill cancerous cells due to the mechanical force they exert on cancerous cells under an external magnetic field [51]. However, in BMNPs, as in our case, the magnetic properties of magnetic MNPs are enhanced compared to monometallic forms [51,52]. So, this study unlocked a facile, cheap, clean, and sustainable approach to preparing magnetic BMNPs to exploit their enhanced magnetic properties in magnetics and the medicinal field.

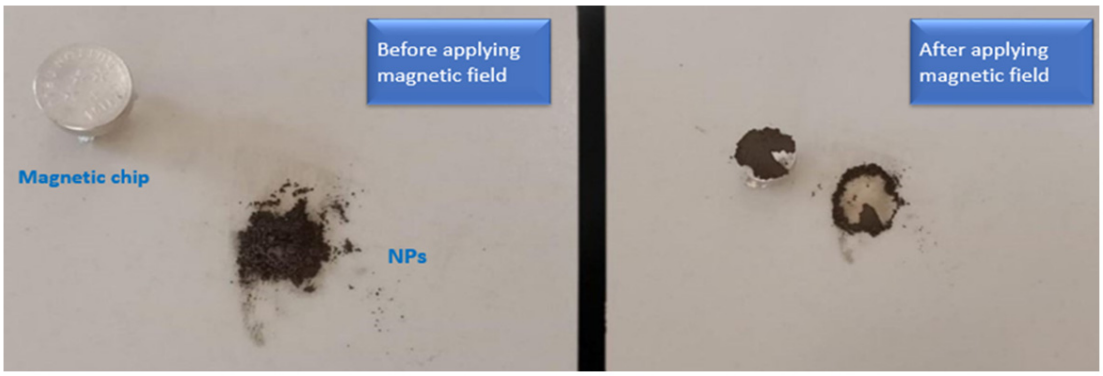

Figure 4. Magnetic assay.

3.2. Phytotoxicity Assay

Although NPs and plant extracts containing compounds have revolutionized medicinal and industrial fields, they also have serious side effects on the environment, especially plants in the environment, which are directly or indirectly susceptible to them in terms of water pollution by industrial discharge. They harm plants in terms of inhibition of seed germination, root elongation, reduction in chlorophyll content, etc., due to their very easy diffusion into plants' cells due to their nano sizes [53,54]. So, in the current work, before diving into finding biological activities, the phytotoxicity of the NPs and the extract was measured to keep in mind their eco-toxicity while using them at the commercial stage and finally taking appropriate preventive measures. So, blank seeds placed under normal conditions showed 100% germination. However, seeds grown with extract and NPs in a phytotoxic kit showed 40% germination (Figure 5a, Table 2). So, %inhibition remained at 60%, and the IC_{50} value was 83.33 mg/mL for both the NPs and the extract (Figure 5b, Table 1). The research findings indicate that despite the eco-toxicity for nanoparticles (NPs) and extracts staying at 60%, the high IC_{50} value implies a low level of eco-toxicity.

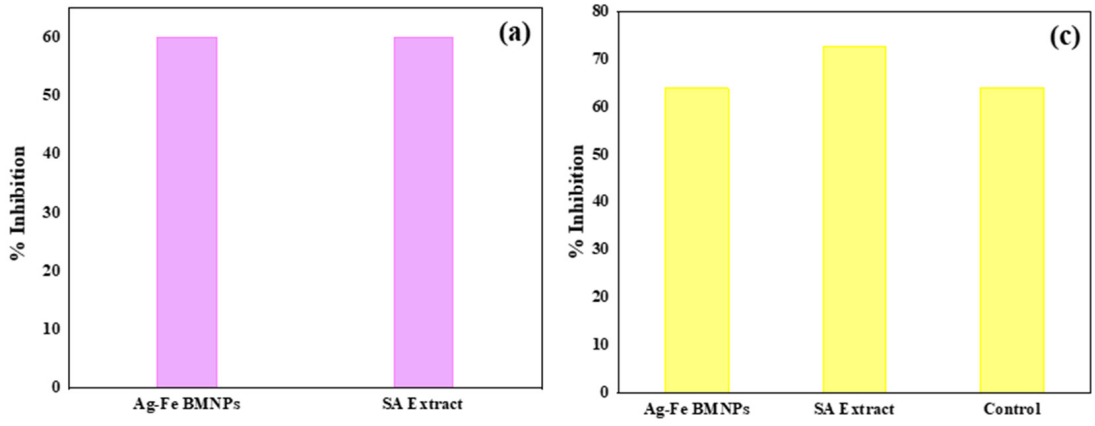

Figure 5. *Cont.*

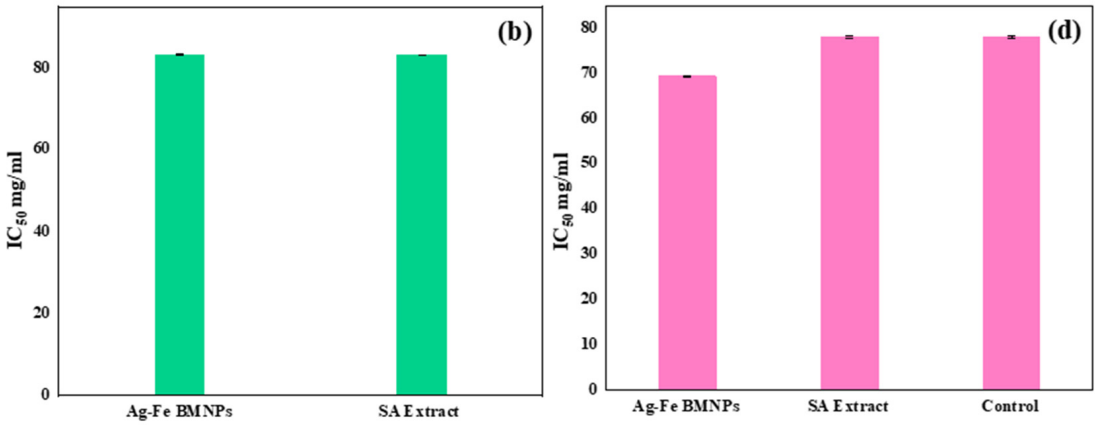

Figure 5. % Inhibition (**a**), IC_{50} pattern (**b**) of phytotoxic assay and % inhibition (**c**) IC_{50} (**d**) of antioxidant assay of NPs and extract, respectively.

Table 2. Phytotoxic assay.

Samples	IC_{50} (mg/mL)	% Inhibition
Ag–Fe BMNPs	83.333 ± 0.089	60
SA Extract	83.333 ± 0.012	60
Positive Control	0	0

3.3. Antioxidant Activities

Free radicals are atoms that are either independent or in molecules with an odd number of electrons and, thus, are very unstable species. So, they stabilize themselves either by gaining or losing electrons when they find the opportunity to do so, and antioxidants stabilize them by providing electrons. In humans, free radicals are produced during normal metabolic processes. Their smaller amount is essential for cellular processes, but their higher amount causes oxidative stress, which makes humans prone to many medical conditions, and one among them is gene mutation [55,56]. So, there is an urgent need to develop benign, cost-effective antioxidants to solve this problem. The antioxidant potential of the NPs and extract was confirmed when, upon their addition to their respective DPPH solutions, the solution changed from deep violet to yellow. The percentage inhibition or radical absorption capability was 64%. 72.74%, and 64% (Figure 5c, Table 3), while IC_{50} (mg/mL) values were 69.48 ± 0.12, 72.12 ± 0.22, and 72.12 ± 0.26 (Figure 5d, Table 3) for NPs, extract, and control, respectively. The results show that the radical absorption percentage of the extract is higher than that of the control, while for NPs, it is equal to that of the control, and theIC_{50} value of the extract is equal to that of the control, while for NPs it is nearly 3 mg/mL less than that of control, indicating that their radical absorption capability is roughly equal to the control, an antioxidant made through conventional methods. Thus, the results suggest that the NPs and the extracts would be suitable substitutes for traditional antioxidants in terms of sustainability.

Table 3. Antioxidant assay.

Samples	IC_{50} (mg/mL)	% Inhibition
Ag–Fe BMNPs	69.48 ± 0.12	64
SA Extract	78.12 ± 0.22	72.77
Positive Control	78.12 ± 0.26	64

3.4. Insecticidal Activities

The world's growing population and its demand for food has emphasized the importance of optimizing agricultural procedures to minimize crop loss. Farmers inevitably suffer crop loss due to several pests, and one among them is insects. Insecticides are widely

used in various fields, especially in the agricultural field. These insecticides require the urgent development of their alternatives due to their growing number of resistant strains towards conventional insecticides and the toxic effects that these insecticides, prepared through conventional routes, leave behind in the environment and have on humans' lives. So, insecticides prepared through bio-routes are very efficient alternatives in terms of the safety of the environment and human health. A lot of work has already been done in this regard earlier. So, in this attempt, we also tried to find the insecticidal potential of our extract and prepared NPs. SA extract killed all of the 10 beetles, showing 100% insecticidal potential or % inhibition or %mortality; Ag–Fe BMNPs killed eight beetles, showing 80% inhibition; and the control killed nine beetles out of 10, showing 90% inhibition (Figure 6a, Table 4). The IC_{50} (mg/mL) value was 56.25, 45, 50 (Figure 6b, Table 4) for the NPs, extract, and control, showing that it is less for the extract and 6 mg/mL higher for the NPs than that of the control So, we developed very efficient Ag–Fe BMNPs and SA extract that exhibited excellent insecticidal activity, confirming that the NPs and the extract would be better alternatives as compared to conventional insecticides, protecting humans, agricultural crops, and the environment from their toxic effects. The Ag–Fe BMNPs and the SA extract showed antibacterial activities against all strains of bacteria (Table 5).

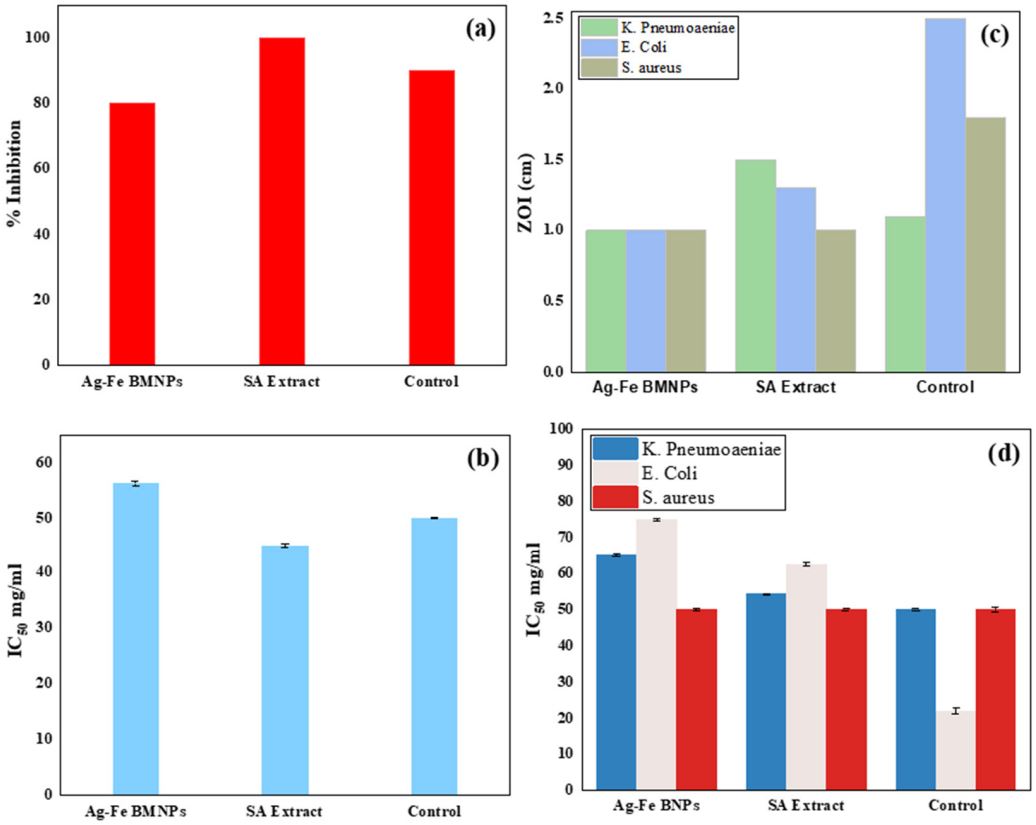

Figure 6. % Inhibition (**a**), IC_{50} (**b**) of insecticidal assay and ZOI (**c**) and IC_{50} (**d**) of antibacterial assay of NPs and extract, respectively.

Table 4. Insecticidal assay.

Samples	IC_{50} (mg/mL)	% Inhibition	Dead/Alive
Ag–Fe BMNPs	56.25 ± 0.41	80	8/2
SA Extract	45 ± 0.24	100	10/0
Positive Control	50 ± 0.14	90	9/1

Table 5. Antibacterial assay in terms of ZOI.

Sample (Concentration)	*K. pneumoaeniae* ZOI (cm)	*E. coli* ZOI (cm)	*S. aureus* ZOI (cm)
Ag–Fe BMNPs (50 µg/mL)	0.59	0.59	0.56
SA Extract (50 µg/mL)	0.8	0.67	0.43
Positive Control (50 µg/mL)	0.8	1.5	1
Ag–Fe BMNPs (100 µg/mL)	1	1	1
SA Extract (100 µg/mL)	1.5	1.3	1
Positive control (100 µg/mL)	1.1	2.5	1.8

Antibacterial Activities

The results show that when the concentration of NPs and extract, against all of the bacterial species, is increased, i.e., from 50 µg/mL to 100 µg/mL, there is also an increase in the ZOI, indicating that the higher the amount of extract and NPs, the higher is their antibacterial activity (Table 5).

The results (Table 4, Figure 6c) also show that the ZOI of SA extract is higher than that of Ag–Fe BMNPs, indicating that the antibacterial activity possessed by the SA extract is higher than that of the NPs. Further, the ZOI of the NPs and extract is lower than that of the positive control, showing that the antibacterial activity of the NPs and the extract is lower than that of the positive control [57]. However, their antibacterial activity is not much lower than that of the positive control, as it is very close to the control in the case of *K. pneumoaeniae*, and half as close to the positive control in the case of *E. coli* and *S. aureus*.

It is clearly shown that the IC_{50} values (Table 6, Figure 6d) were higher for both the extract and the NPs (and the value of the NPs was even higher than that of the extract) as compared to the control against *K. pneumoaeniae* and *E. coli* and equal to that of control in the case of *S. aureus*.

Table 6. Antibacterial assay in terms of IC_{50} values.

Samples	*K. pneumoaeniae* IC_{50} (mg/mL)	*E. coli* IC_{50} (mg/mL)	*S. aureus* IC_{50} (mg/mL)
Ag–Fe BMNPs	65 ± 0.29	75 ± 0.29	50 ± 0.31
SA Extract	54.16666667 ± 0.29	62.5 ± 0.37	50 ± 0.40
Positive Control	50 ± 0.21	22 ± 0.71	50 ± 0.57

In short, the results suggest that the NPs and the extract are better substitutes for traditional antibiotics, like cefixime, in terms of sustainability and bacterial resistance, i.e., they are easy to make, cost-effective, environmentally friendly, less time-consuming in their synthesis, produce less waste, require less energy, and easily handled conditions for their synthesis. The results confirm the powerful antibacterial potential of NPs as an extract, although the ZOI was lower for them as compared to the control; on the other hand, the IC_{50} values were higher for them than they were for the control, suggesting that they would be the best substitute for antimicrobial agents in future.

3.5. Mechanism of Antibacterial Activity of Ag–Fe BMNPs

Due to the growing number of antibiotic-resistant strains, scientists are making ongoing efforts to find alternatives. Among these alternatives, metal nanoparticles are anticipated to be best due to their capability to poison many biomolecules in bacterial cells in one go before they develop resistance. NPs' diminutive size makes them capable of efficiently diffusing inside the cells and showing their magic. A lot of studies have revealed that they kill bacteria in a variety of ways (Figure 7, Table 7), and a highly debated way is by their reaction with mitochondrial enzymes, causing the creation of reactive oxygen species (ROS) [11,24,58]. This causes oxidative stress in various ways, such as by causing gene mutation due to DNA disruption, loss of tertiary and secondary structure of enzymes

and proteins, and disruption of ion channel of the cell membrane, causing the leakage of cytoplasmic contents, etc.

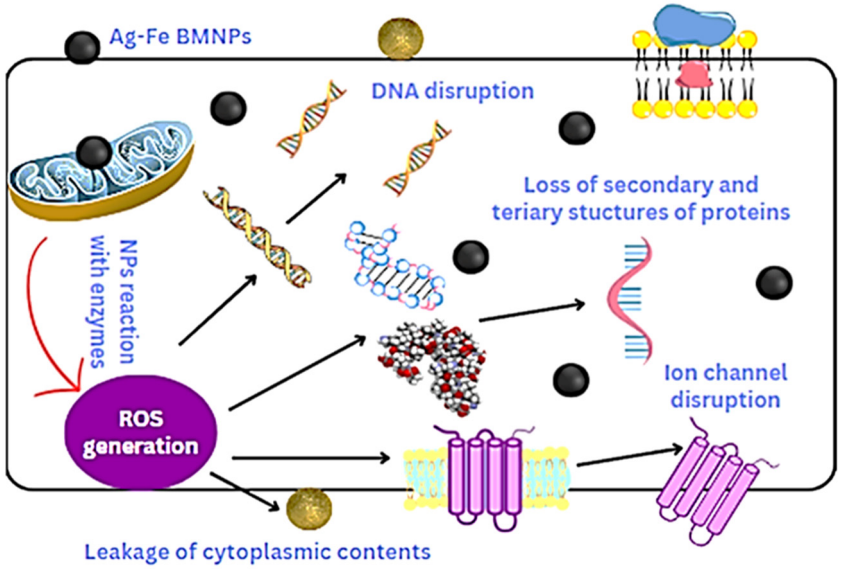

Figure 7. Antibacterial mechanism of NPs.

Table 7. Table of comparison of the current work with previous literature.

Study Focus	Synthesis Method	Nanoparticle Source	Characterization Techniques	Applications	Catalytic/Biological Efficacy	References
Ag–Fe BMNPs using *Syzygium aromaticum*	Green synthesis with plant extract	$AgNO_3$ and $FeNO_3.9H_2O$	UV-VIS, XRD, EDX, FTIR, SEM	Antioxidant, antibacterial, insecticidal	Antioxidant: 64–73% inhibition; Antibacterial: 1–1.5 cm ZOI; Insecticidal: 80–100% mortality	This work
Ag–Fe BMNPs using Salvia officinalis	Green synthesis with plant extract	$AgNO_3$ and $Fe(NO_3)_3$	UV-VIS, TEM, SEM, XRD, FTIR, EDX, TGA	Catalytic degradation of 4-nitrophenol	Efficient reduction of 4-Nitrophenol to 4-Aminophenol	[59]
Ag–Fe BMNPs using Gardenia jasminoides	Green synthesis with plant extract	Ag and Fe salts	UV-VIS, SEM	Antimicrobial against multidrug-resistant strains	Exhibited antimicrobial (bactericidal) synergistic effect	[24]
Ag@Fe BMNPs using Palm dates fruit	Green synthesis with fruit extract	$AgNO_3$ and $Fe(NO_3)_3$	UV-VIS, TEM, EDX	Antioxidant, antimicrobial, photocatalytic	Good in vitro antibacterial activity; used as catalyst for degradation of bromothymol blue	[48]
Ag–Fe BMNPs using Papaya leaf extract	Green synthesis with plant extract	Ag and Fe salts	UV-VIS, FT-IR	Antimicrobial	Effective antibacterial activity on pathogenic bacteria	[60]
Ag–Fe BMNPs using Beta vulgaris L.	Green synthesis with plant extract	Ag and Fe salts	UV-VIS, FTIR, SEM, TEM, EDX	Antifungal, induces apoptosis in fungal cells	Induces apoptosis and cell cycle arrest in Candida auris	[60]
Ag–Fe BMNPs using Passiflora edulis	Green synthesis with plant extract	Ag and Fe salts	UV-VIS, XRD, SEM	Antimicrobial, antioxidant	Demonstrated effective antibacterial and antifungal activities; high antioxidant activity	[61]

4. Experimental

4.1. Chemicals

All the used chemicals, $AgNO_3$, $FeNO_3.9H_2O$, DPPH, Cefixime, and Cypermethrin, were of analytical grade and bought from a local supplier. Deionized water was used to make all solutions during the whole study. Bud extract of *Syzygium aromaticum* (SA) used to make extract and maize seeds used for phytotoxic assay, were bought from the local market.

4.2. Preparation of SA Bud Extract

SA buds were washed thoroughly, dried, and ground to powder. Then, 5 g of cloves powder was taken into 200 mL of hot deionized water and heated with stirring for 30 min at 60 °C. The mixture was cooled at room temperature and filtered with Whatman filter paper No. 1. The filtrate was kept in a freezer at 4 °C.

4.3. Preparation of Ag–Fe BMNPs

Next, 0.01 M $AgNO_3$ and $FeNO_3{\cdot}9H_2O$ solutions were prepared in deionized water. Both solutions were mixed and heated at 80 °C for 10 min, along with stirring. A total of 10 mL of the SA extract was added to the reaction solution. The solution's color changed dramatically from golden yellow to jet black, indicating the creation of BMNPs. The solution was allowed to heat at 80 °C for 1 h. The jet-black colored solution was centrifuged at 400 rpm for 5 min and washed with deionized water and dried at 80 °C for 23 h (Figure 8).

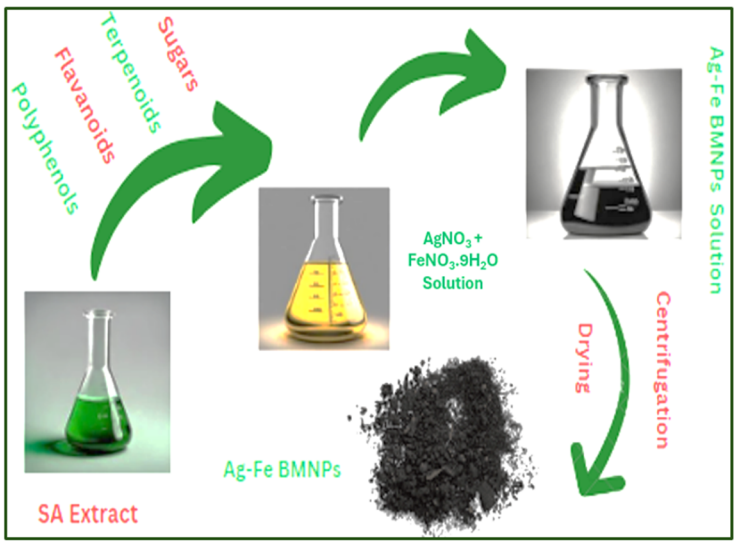

Figure 8. Schematic representation of Ag–Fe NP synthesis.

4.4. Characterizations

The as-prepared Ag–Fe BMNPs were analyzed using analytical techniques. Agilent Cary 60 UV-VIS spectrophotometer (Agilent, Penang, Malaysia), 200–600 nm range, was used to examine the optical properties and preliminary evaluation of the reaction. Agilent Cary 360 FTIR spectrophotometer (Agilent, Penang, Malaysia), 4000–600 cm^{-1} range, was used to see the functionalities present in biomolecules for creating and stabilizing NPs. D2 Phaser Bruker XRD (Bruker AXS, Karlsruhe, Germany) with CuKα radiations (λ = 1.54 Å, 45 kV, 40 mA), 25–80° range (scan rate, 0.02 min^{-1}), was used to study crystallinity and size of BMNPs. Nova Nano SEM 450 FE-SEM (Thermo Fisher, New York, NY, USA) was used to check the surface morphology and the same instrument was used for EDX analysis to find the elemental constitution.

4.5. Applications

4.5.1. Magnetic Studies

A magnetic chip was brought closer to Ag–Fe BMNPs to observe their magnetism. The magnetic chip was used to produce the magnetic field. The attraction of BMNPs toward the chip showed magnetic characteristics and confirmed the core–shell structure of BMNPs. A similar experiment was performed by Sher et al. in 2021 [62].

4.5.2. Biological Studies

Biological assays were made for Ag–Fe BMNPs and SA extract. Their potential for biological activities was checked by comparing it with that of control. Biological studies were made in two parts: by calculation of (a) %inhibition or zone of inhibition (ZOI), with greater %inhibition or ZOI correlating to greater biological activity and vice-versa; and (b) IC_{50} values [24], with smaller IC_{50} value correlating to greater biological activity and vice versa [63]. The IC_{50} value for NPs and extract was calculated from the graph of %age inhibition or ZOI versus sample concentration in every biological activity.

4.5.3. Phytotoxic Assay

The phytotoxic assay of Ag–Fe BMNPs and SA extract was performed using maize seeds [64]. The seeds were immersed in sodium hypochlorite solution (0.1%) for 10 min for sterilization, and further soaked in distilled water for 10 min. Then, 10 seeds were placed inside the phytotoxic kit containing Ag–Fe BMNPs with a distance of 2 cm between each seed, and the kit was placed in an incubator at room temperature. Growth germination was noted after one day. Control seeds showed 100% germination. The germination rate or % age inhibition of seed growth was calculated using the following equation:

$$\%\text{inhibition} = (\text{NO. of non} - \text{germinated seeds/initial No. of seeds}) * 100$$

Lastly, the IC_{50} of NPs and extract was also calculated.

4.5.4. Antioxidant Assay

Antioxidant studies of Ag–Fe BMNPs and SA extract were checked by performing a DPPH assay according to Shahzad et al. [65]. First, 1 mL of freshly prepared DPPH methanolic solution (0.004%) was added into 3 mL of Ag–Fe BMNPs (50 mg/mL and 100 mg/mL), mixed thoroughly, and placed the mixture in the dark for 30 min, and absorbance was taken at 517 nm. Ascorbic acid was used as a standard here. Then, % inhibition, (DPPH radical capturing potential) was calculated using the following equation:

$$\%\text{age inhibition} = (\text{standard's absorbance} - \text{sample's absorbance/standard's absorbance}) * 100$$

4.5.5. Insecticidal Assay

The insecticidal potential of Ag–Fe BMNPs and SA extract was performed using red beetles as model insects. The samples of 0.5 mg/mL, 1 mg/mL, and 1.5 mg/mL were added to three labeled petri dishes and placed in an incubator to dry. After drying, 10 red beetles were added to each petri dish to evaluate the insecticidal potential of extract and NPs. The highest and lowest doses of samples were used to calculate lethal concentration. Cypermethrin was used as a positive control. Next, %age mortality or %age inhibition, showing the insecticidal potential of test sample and extract, was found using the following equation:

$$\%\text{age mortality} = (\text{NO. of dead beetles/initial NO. of live beetles}) * 100$$

4.5.6. Antibacterial Assay

The antibacterial potential of Ag–Fe BMNPs and SA extract was checked against *K. pneumoniae*, *S. aureus*, and *E. coli* using the disc diffusion method. A filtered disc (6 mm in diameter) of 100 microliters suspension of each bacterial species; 10^7 colony-forming units (CFU/mL) were made and injected into their respective petri dish containing agar

nutrients. Each filtered disc was saturated with BMNPs and placed at 4 °C for 2 h, followed by incubation at 37 °C for 18 h. The measurement of ZOI, followed by IC_{50} calculation was performed. Cefixime was used as a positive control.

4.6. Statistical Analysis

All biological assays were performed in triplicate, and results are shown as their mean values. All of the experimental calculations were performed using MS Excel 2018.

5. Conclusions

In this study, we have produced core–shell Ag–Fe BMNPs using the bud extract of *S. aromaticum*, which was confirmed by their characteristic SPR peak obtained by their UV-VIS analysis. Phyto-molecules, present in the SA extrac and responsible for the creation and stabilization of NPs, were confirmed by FTIR. The average crystalline size of NPs, calculated by the Scherrer equation using XRD data, is 16 nm. The SEM image clearly shows that the NPs are nearly spherical. The prepared NPs and extracts were evaluated to check their antibacterial, antioxidant, and insecticidal activities as compared with the control. The results have shown that they possess either higher or comparable activities to those of control, suggesting them as the best possible alternatives to traditional antibiotics, antioxidants, and insecticides made through primitive methods. We have produced them using a simple, facile, inexpensive, one-vessel, and one-step process taking only one hour, at 80 °C using eco-safe deionized water as a solvent, from preparing the extract and the NPs to their applications at all stages of research work. Further, the equipment used for their synthesis is also not very expensive compared to the equipment used in their conventional synthesis, a step towards sustainable development. Our study paves the way towards sustainable development and applications of Ag–Fe BMNPs in medicinal and agricultural fields, demanding further research on their use in antioxidant, insecticidal, and antibacterial formulations.

Author Contributions: Conceptualization, M.A.Q.; methodology, F.M. and N.A.; validation, N.S.B., A.Y., I.K. and M.I.; formal analysis, M.A.Q., M.S.A., I.K., B.R.P. and M.I.; investigation, N.A., S.U.-D.K., N.S.B. and I.K.; data curation, A.Y., A.A.C., N.S.B. and M.S.A.; writing—original draft preparation, F.M. and M.A.Q.; writing—review and editing, M.A.Q., N.A., A.Y., A.A.C., S.U.-D.K., N.A.I., B.R.P. and M.I.; visualization, A.Y. and A.A.C.; supervision, N.A.; funding acquisition, N.A.I. All authors have read and agreed to the published version of the manuscript.

Funding: Imam Mohammad Ibn Saud Islamic University (IMSIU) (grant number IFP-IMSIU-2023058).

Data Availability Statement: The original contributions presented in the study are included in the article, further inquiries can be directed to the corresponding authors.

Acknowledgments: This work was supported and funded by the Deanship of Scientific Research at Imam Mohammad Ibn Saud Islamic University (IMSIU) (grant number IFP-IMSIU-2023058).

Conflicts of Interest: The authors declare no conflicts of interest.

References

1. Puri, A.; Mohite, P.; Maitra, S.; Subramaniyan, V.; Kumarasamy, V.; Uti, D.E.; Sayed, A.A.; El-Demerdash, F.M.; Algahtani, M.; El-Kott, A.F. From nature to nanotechnology: The interplay of traditional medicine, green chemistry, and biogenic metallic phytonanoparticles in modern healthcare innovation and sustainability. *Biomed. Pharmacother.* **2024**, *170*, 116083. [CrossRef]
2. Javed, F.; Akhter, N.; Qamar, M.A.; Yaqoob, A.; Farhan, A.; Shahid, M.; Shariq, M.; Nazir, M.; Khan, Z. Biogenic derived cobalt nanoparticles using *Morus alba* and their potent antibacterial and catalytic degradation activity. *Chem. Pap.* **2024**, *78*, 3137–3147. [CrossRef]
3. Rashid, A.B.; Haque, M.; Islam, S.M.; Labib, K.R.U. Nanotechnology-enhanced fiber-reinforced polymer composites: Recent advancements on processing techniques and applications. *Heliyon* **2024**, *10*, e24692. [CrossRef]
4. Chatterjee, R.; Sarkar, S.; Dutta, A.K.; Akinay, Y.; Dasgupta, S.; Mukhopadhyay, M. Scope and Challenges for Green Synthesis of Functional Nanoparticles. In *Novel Applications of Carbon Based Nano-Materials*; CRC Press: Boca Raton, FL, USA, 2022; pp. 274–318.
5. Balasubramanian, S.; Gurumurthy, B.; Balasubramanian, A. Biomedical applications of ceramic nanomaterials: A review. *Int. J. Pharm. Sci. Res.* **2017**, *8*, 4950–4959.

6. Ahmed, S.; Ansari, A.; Siddiqui, M.A.; Ranjan, P. Metal/Polymeric Hierarchical platform as biosensor. In Proceedings of the International Conference on Nanotechnology: Opportunities and Challenges, New Delhi, India, 28–29 November 2022; pp. 17–24. Available online: https://search.app/JQob5Pqhe9mknX6K8 (accessed on 21 March 2024).
7. Ali, S.K.; Alamier, W.M.; Hasan, N.; Ahmed, S.; Ansari, A.; Imran, M. Synergistic nanomaterials: Zinc sulfide-polyaniline for ciprofloxacin electrochemical sensing. *Appl. Phys. A* **2023**, *129*, 859. [CrossRef]
8. Liu, X.; Zheng, W.; Kumar, R.; Kumar, M.; Zhang, J. Conducting polymer-based nanostructures for gas sensors. *Coord. Chem. Rev.* **2022**, *462*, 214517. [CrossRef]
9. Khan, A.; Ahmed, S.; Sun, B.-Y.; Chen, Y.-C.; Chuang, W.-T.; Chan, Y.-H.; Gupta, D.; Wu, P.-W.; Lin, H.-C. Self-healable and anti-freezing ion conducting hydrogel-based artificial bioelectronic tongue sensing toward astringent and bitter tastes. *Biosens. Bioelectron.* **2022**, *198*, 113811. [CrossRef] [PubMed]
10. Javed, M.; Iqbal, S.; Qamar, M.A.; Shariq, M.; Ahmed, I.A.; BaQais, A.; Alzahrani, H.; Ali, S.K.; Masmali, N.; Althagafi, T.M. Fabrication of effective Co-SnO_2/sgcn photocatalysts for the removal of organic pollutants and pathogen inactivation. *Crystals* **2023**, *13*, 163. [CrossRef]
11. Sher, M.; Khan, S.A.; Shahid, S.; Javed, M.; Qamar, M.A.; Chinnathambi, A.; Almoallim, H.S. Synthesis of novel ternary hybrid g-C_3N_4@ Ag-ZnO nanocomposite with Z-scheme enhanced solar light-driven methylene blue degradation and antibacterial activities. *J. Environ. Chem. Eng.* **2021**, *9*, 105366. [CrossRef]
12. Greten, L.; Salzwedel, R.; Katzer, M.; Mittenzwey, H.; Christiansen, D.; Knorr, A.; Selig, M. Dipolar coupling at interfaces of ultrathin semiconductors, semimetals, plasmonic nanoparticles, and molecules. *Phys. Status Solidi* **2024**, *221*, 2300102. [CrossRef]
13. Abutaleb, A.; Ahmed, S.; Imran, M. Synergistic photocatalysis: Harnessing WSe_2-ZnO nanocomposites for efficient malachite green dye degradation. *Eur. Phys. J. Plus* **2023**, *138*, 1046. [CrossRef]
14. Ahmed, S.; Ansari, A.; Siddiqui, M.A.; Ranjan, P.; Kumar, P. Catalysts for Li-S batteries. In *Single Atom Catalysts*; Elsevier: Amsterdam, The Netherlands, 2024; pp. 215–231.
15. Reddy, M.S.B.; Aich, S. Recent progress in surface and heterointerface engineering of 2D MXenes for gas sensing applications. *Coord. Chem. Rev.* **2024**, *500*, 215542. [CrossRef]
16. Chugh, R.; Kaur, G. A mini review on green synthesis of nanoparticles by utilization of Musa-balbisiana waste peel extract. *Mater. Today Proc.* **2022**. Available online: https://www.sciencedirect.com/science/article/pii/S2214785322070390?via=ihub (accessed on 21 March 2024). [CrossRef]
17. Wenderich, K.; Mul, G. Methods, mechanism, and applications of photodeposition in photocatalysis: A review. *Chem. Rev.* **2016**, *116*, 14587–14619. [CrossRef]
18. Ahmad, K.; Raza, W.; Khan, M.Q. Water splitting: Design, synthesis and fabrication of nanostructured materials based efficient electrodes for water splitting applications. In *Handbook of Greener Synthesis of Nanomaterials and Compounds*; Elsevier: Amsterdam, The Netherlands, 2021; pp. 549–564.
19. Roy, S.; Das, T.K. Plant mediated green synthesis of silver nanoparticles—A review. *Int. J. Plant Biol. Res* **2015**, *3*, 1044–1055.
20. Rani, N.; Singh, P.; Kumar, S.; Kumar, P.; Bhankar, V.; Kumar, K. Plant-mediated synthesis of nanoparticles and their applications: A review. *Mater. Res. Bull.* **2023**, 112233. [CrossRef]
21. Zaka, M.; Abbasi, B.H. Effects of bimetallic nanoparticles on seed germination frequency and biochemical characterisation of Eruca sativa. *IET Nanobiotechnol.* **2017**, *11*, 255–260. [CrossRef] [PubMed]
22. Kang, C.-W.; Kolya, H. Green synthesis of Ag-Au bimetallic nanocomposites using waste tea leaves extract for degradation congo red and 4-Nitrophenol. *Sustainability* **2021**, *13*, 3318. [CrossRef]
23. Zaib, M.; Malik, T.; Akhtar, N.; Shahzadi, T. Sensitive detection of sulphide ions using green synthesized monometallic and bimetallic nanoparticles: Comparative study. *Waste Biomass Valorization* **2022**, *13*, 2447–2459. [CrossRef]
24. Padilla-Cruz, A.; Garza-Cervantes, J.; Vasto-Anzaldo, X.G.; García-Rivas, G.; León-Buitimea, A.; Morones-Ramírez, J. Synthesis and design of Ag–Fe bimetallic nanoparticles as antimicrobial synergistic combination therapies against clinically relevant pathogens. *Sci. Rep.* **2021**, *11*, 5351. [CrossRef]
25. Mohan, S.; Devan, M.V.; Sambathkumar, S.; Shanmugam, V.; Ravikumar, K.; Marnadu, R.; Palanivel, B.; Hegazy, H. Dual probes of Ag/Pd bimetallic NPs facilely synthesized by green process using Catharanthus leaf extract on textile dye removal and free radical capability. *Appl. Nanosci.* **2021**, *11*, 1565–1574. [CrossRef]
26. Qamar, M.A.; Javed, M.; Shahid, S.; Sher, M. Fabrication of g-C_3N_4/transition metal (Fe, Co, Ni, Mn and Cr)-doped ZnO ternary composites: Excellent visible light active photocatalysts for the degradation of organic pollutants from wastewater. *Mater. Res. Bull.* **2022**, *147*, 111630. [CrossRef]
27. Hasan, A.; Morshed, M.; Memic, A.; Hassan, S.; Webster, T.J.; Marei, H.E.-S. Nanoparticles in tissue engineering: Applications, challenges and prospects. *Int. J. Nanomed.* **2018**, *13*, 5637–5655. [CrossRef] [PubMed]
28. Nikiema, W.A.; Ouédraogo, M.; Ouédraogo, W.P.; Fofana, S.; Ouédraogo, B.H.A.; Delma, T.E.; Amadé, B.; Abdoulaye, G.M.; Sawadogo, A.S.; Ouédraogo, R. Systematic Review of Chemical Compounds with Immunomodulatory Action Isolated from African Medicinal Plants. *Molecules* **2024**, *29*, 2010. [CrossRef] [PubMed]
29. Dwinandha, D.; Elsamadony, M.; Gao, R.; Fu, Q.-L.; Liu, J.; Fujii, M. Interpretable Machine Learning and Reactomics Assisted Isotopically Labeled FT-ICR-MS for Exploring the Reactivity and Transformation of Natural Organic Matter during Ultraviolet Photolysis. *Environ. Sci. Technol.* **2023**, *58*, 816–825. [CrossRef] [PubMed]

30. Aslam, B.; Ahmad, M.; Tariq, M.U.; Muzammil, S.; Siddique, A.B.; Khurshid, M.; Shahid, A.; Rasool, M.H.; Chaudhry, T.H.; Amir, A. Antibiotic resistance: Retrospect and prospect. In *Degradation of Antibiotics and Antibiotic-Resistant Bacteria from Various Sources*; Elsevier: Amsterdam, The Netherlands, 2023; pp. 1–37.
31. Semaltianos, N. Nanoparticles by laser ablation. *Crit. Rev. Solid State Mater. Sci.* **2010**, *35*, 105–124. [CrossRef]
32. Nyabadza, A.; Vazquez, M.; Brabazon, D. A review of bimetallic and monometallic nanoparticle synthesis via laser ablation in liquid. *Crystals* **2023**, *13*, 253. [CrossRef]
33. Murugadoss, A.; Kai, N.; Sakurai, H. Synthesis of bimetallic gold–silver alloy nanoclusters by simple mortar grinding. *Nanoscale* **2012**, *4*, 1280–1282. [CrossRef] [PubMed]
34. Li, Q.; Yang, S.; Wu, S.; Fan, D. Mechanochemically synthesized Al–Fe (oxide) composite with superior reductive performance: Solid-state kinetic processes during ball milling. *Chemosphere* **2022**, *298*, 134280. [CrossRef]
35. Tungare, K.; Bhori, M.; Patil, S.A.; Iyer, P.; Jagtap, N.; Kadam, A.; Vijayakuma, S. Clove Buds (Syzygium aromaticum). In *Medicinal Spice and Condiment Crops*; CRC Press: Boca Raton, FL, USA, 2024; pp. 200–224.
36. Palem, V.V.; Paramasivam, G.; Dey, N.; Ananthan, A.S. Processes of Synthesis and Characterization of Silver Nanoparticles with Antimicrobial Action and their Future Prospective. *Nanobiomater. Perspect. Med. Appl. Diagn. Treat. Dis.* **2023**, *145*, 131–161.
37. Daramola, O.B.; George, R.C.; Torimiro, N.; Olajide, A.A. Insights on the synthesis of iron-oxide nanoparticles and the detection of iron-reducing genes from soil microbes. *Colloids Surf. C Environ. Asp.* **2024**, *2*, 100025. [CrossRef]
38. Shilpa, M.; Shetty, V.; Surabhi, S.; Jeong, J.-R.; Morales, D.; Ballal, M.; Eshwarappa, K.; Murari, M.; Nayak, R.; Gurumurthy, S. Decentralized core-shell Au/Ag bimetallic nanostructures prepared via green approach for catalytic and antimicrobial applications. *Mater. Sci. Eng. B* **2023**, *298*, 116893. [CrossRef]
39. Sarani, M.; Hamidian, K.; Barani, M.; Adeli-Sardou, M.; Khonakdar, H.A. α-Fe_2O_3@ Ag and Fe_3O_4@ Ag Core-Shell Nanoparticles: Green Synthesis, Magnetic Properties and Cytotoxic Performance. *ChemistryOpen* **2023**, *12*, e202200250. [CrossRef] [PubMed]
40. Sudhakar, C.; Selvam, K.; Poonkothai, M.; Ranjitha, S. Biomimetic synthesis of Ag@ Fe bimetallic nanoparticles from Palmyra sprouts extract and their antibacterial, photocatalytic degradation of malachite green. *Inorg. Chem. Commun.* **2024**, *161*, 112132. [CrossRef]
41. Qamar, M.A.; Shahid, S.; Javed, M.; Iqbal, S.; Sher, M.; Akbar, M.B. Highly efficient g-C_3N_4/Cr-ZnO nanocomposites with superior photocatalytic and antibacterial activity. *J. Photochem. Photobiol. A Chem.* **2020**, *401*, 112776. [CrossRef]
42. Teng, Y.; Bian, X.; Fu, X.; Song, Y.; Bai, X. Effect of Iron Component on the Structural Evolution of Carbon Bonds in Hydrochloric Acid-Demineralized Lignite During Pyrolysis. *ACS Omega* **2023**, *8*, 17634–17643. [CrossRef] [PubMed]
43. Ghosh, S.; Roy, S.; Naskar, J.; Kole, R.K. Plant-mediated synthesis of mono-and bimetallic (Au–Ag) nanoparticles: Future prospects for food quality and safety. *J. Nanomater.* **2023**, *2023*, 2781667. [CrossRef]
44. Freire, T.M.; Freire, R.M.; Franco, M.L.; López, E.O.; de Oliveira, R.C.; Denardin, J.C.; Oliveira, F.G.S.; Vasconcelos, I.F.; Casciano, P.N.S.; de Lima-Neto, P.; et al. Magnetic FeM (M= Ag, Co, Cu, and Ni) nanocrystals as electrocatalysts for hydrogen evolution reaction. *Mater. Today Sustain.* **2022**, *18*, 100150. [CrossRef]
45. Albeladi, A.; Khan, Z.; Al-Thabaiti, S.A.; Patel, R.; Malik, M.A.; Mehta, S. Fe_3O_4-CdO Nanocomposite for Organic Dye Photocatalytic Degradation: Synthesis and Characterization. *Catalysts* **2024**, *14*, 71. [CrossRef]
46. Kaur, N.; Singh, A.; Ahmad, W. Microwave assisted green synthesis of silver nanoparticles and its application: A review. *J. Inorg. Organomet. Polym. Mater.* **2023**, *33*, 663–672. [CrossRef]
47. Ali, S.; Zahid, A.; Shahid, S.T. *Green Engineering of Iron and Iron Oxide Nanoparticles*; IntechOpen: London, UK, 2023. [CrossRef]
48. Al-Asfar, A.; Zaheer, Z.; Aazam, E.S. Eco-friendly green synthesis of Ag@Fe bimetallic nanoparticles: Antioxidant, antimicrobial and photocatalytic degradation of bromothymol blue. *J. Photochem. Photobiol. B Biol.* **2018**, *185*, 143–152. [CrossRef]
49. Sharma, R.; Garg, R.; Bali, M.; Eddy, N.O. Potential applications of green-synthesized iron oxide NPs for environmental remediation. *Environ. Monit. Assess.* **2023**, *195*, 1397. [CrossRef] [PubMed]
50. Sithara, N.; Bharathi, D.; Lee, J.; Mythili, R.; Devanesan, S.; AlSalhi, M.S. Synthesis of iron oxide nanoparticles using orange fruit peel extract for efficient remediation of dye pollutant in wastewater. *Environ. Geochem. Health* **2024**, *46*, 30. [CrossRef] [PubMed]
51. Dolai, J.; Ray, R.; Ghosh, S.; Maity, A.; Jana, N.R. Optical Nanomaterials for Advanced Bioimaging Applications. *ACS Appl. Opt. Mater.* **2023**, *2*, 1–14. [CrossRef]
52. Nanda, S.S.; Yi, D.K. Recent Advances in Synergistic Effect of Nanoparticles and Its Biomedical Application. *Int. J. Mol. Sci.* **2024**, *25*, 3266. [CrossRef] [PubMed]
53. Saranya, R.; Yashoda, R.H.; Nargund, V.B.; Basavaraj, T.; Dinesh, K.; Varsha, S.L.; Vinay, J.U.; Chidanandappa, E.; Srikanth, H.N. In vitro evaluation of green nanoparticles against Ceratocystis fimbriata and Fusarium oxysporum causing wilt disease of pomegranate. *Indian Phytopathol.* **2024**, *77*, 1–8.
54. Hai, N.D.; Huy, N.; Nam, N.T.H.; An, H.; Cong, C.Q.; Dat, N.M.; Vu, N.H.; Truong, N.T.N.; Hieu, N.H. Comparative investigation of the characterization and photoactivity of gold-decorated graphitic carbon nitride: A study aspect of various synthesis approaches. *Surf. Interfaces* **2024**, *44*, 103645. [CrossRef]
55. Bhanja, S.K.; Samanta, S.K.; Mondal, B.; Jana, S.; Ray, J.; Pandey, A.; Tripathy, T. Green synthesis of Ag@ Au bimetallic composite nanoparticles using a polysaccharide extracted from Ramaria botrytis mushroom and performance in catalytic reduction of 4-nitrophenol and antioxidant, antibacterial activity. *Environ. Nanotechnol. Monit. Manag.* **2020**, *14*, 100341. [CrossRef]
56. Velpula, S.; Beedu, S.R.; Rupula, K. Bimetallic nanocomposite (Ag-Au, Ag-Pd, Au-Pd) synthesis using gum kondagogu a natural biopolymer and their catalytic potentials in the degradation of 4-nitrophenol. *Int. J. Biol. Macromol.* **2021**, *190*, 159–169. [CrossRef]

57. Sher, M.; Javed, M.; Shahid, S.; Hakami, O.; Qamar, M.A.; Iqbal, S.; Al-Anazy, M.M.; Baghdadi, H.B. Designing of highly active g-C_3N_4/Sn doped ZnO heterostructure as a photocatalyst for the disinfection and degradation of the organic pollutants under visible light irradiation. *J. Photochem. Photobiol. A Chem.* **2021**, *418*, 113393. [CrossRef]
58. Qamar, M.A.; Shahid, S.; Javed, M.; Sher, M.; Iqbal, S.; Bahadur, A.; Li, D. Fabricated novel g-C_3N_4/Mn doped ZnO nanocomposite as highly active photocatalyst for the disinfection of pathogens and degradation of the organic pollutants from wastewater under sunlight radiations. *Colloids Surf. A Physicochem. Eng. Asp.* **2021**, *611*, 125863. [CrossRef]
59. Malik, M.; Alshehri, A.; Patel, R. Facile one-pot green synthesis of Ag-Fe bimetallic nanoparticles and their catalytic capability for 4-Nitrophenol reduction. *J. Mater. Res. Technol.* **2021**, *12*, 455–470. [CrossRef]
60. Yoro, M.; Ayuba, I. Green Synthesis, Characterization and Antimicrobial Potency of Ag-Fe Bimetallic Nanoparticles from Papaya Leaf Extract. *Int. J. Sci. Res. Publ. (IJSRP)* **2022**, *12*, 563. [CrossRef]
61. Sandupatla, R.; Dongamanti, A.; Koyyati, R. Antimicrobial and antioxidant activities of phytosynthesized Ag, Fe and bimetallic Fe-Ag nanoparticles using Passiflora edulis: A comparative study. *Mater. Today Proc.* **2021**, *44*, 2665–2673. [CrossRef]
62. Kumar, A.; Shah, S.R.; Jayeoye, T.J.; Kumar, A.; Parihar, A.; Prajapati, B.; Singh, S.; Kapoor, D.U. Biogenic metallic nanoparticles: Biomedical, analytical, food preservation, and applications in other consumable products. *Front. Nanotechnol.* **2023**, *5*, 1175149. [CrossRef]
63. Mihailović, V.; Srećković, N.; Nedić, Z.P.; Dimitrijević, S.; Matić, M.; Obradović, A.; Selaković, D.; Rosić, G.; Katanić Stanković, J.S. Green synthesis of silver nanoparticles using Salvia verticillata and Filipendula ulmaria extracts: Optimization of synthesis, biological activities, and catalytic properties. *Molecules* **2023**, *28*, 808. [CrossRef] [PubMed]
64. Rob, M.M.; Hossen, K.; Iwasaki, A.; Suenaga, K.; Kato-Noguchi, H. Phytotoxic activity and identification of phytotoxic substances from Schumannianthus dichotomus. *Plants* **2020**, *9*, 102. [CrossRef]
65. Shahid Chatha, S.; Hussain, A.; Asad, R.; Majeed, M.; Aslam, N. Bioactive components and antioxidant properties of *Terminalia arjuna* L. extracts. *J. Food Process Technol.* **2014**, *5*, 2. [CrossRef]